

O₂ Activation by Non-Heme Diiron Proteins: Identification of a Symmetric μ -1,2-Peroxide in a Mutant of Ribonucleotide Reductase[†]

Pierre Moënne-Loccoz,^{‡,§} Jeffrey Baldwin,^{‡,||} Brenda A. Ley,^{||} Thomas M. Loehr,[§] and J. Martin Bollinger, Jr.*^{*,||}

Department of Biochemistry and Molecular Biology, Oregon Graduate Institute of Science and Technology, Portland, Oregon 97291-1000, and Department of Biochemistry and Molecular Biology, The Pennsylvania State University, University Park, Pennsylvania 16802

Received July 31, 1998; Revised Manuscript Received September 3, 1998

ABSTRACT: Non-heme diiron clusters occur in a number of enzymes (e.g., ribonucleotide reductase, methane monooxygenase, and Δ^9 -stearoyl-ACP desaturase) that activate O₂ for chemically difficult oxidation reactions. In each case, a kinetically labile peroxo intermediate is believed to form when O₂ reacts with the diferrous enzyme, followed by O–O bond cleavage and the formation of high-valent iron intermediates [formally Fe(IV)] that are thought to be the reactive oxidants. Greater kinetic stability of a peroxodiiron(III) intermediate in protein R2 of ribonucleotide reductase was achieved by the iron-ligand mutation Asp84 → Glu and the surface mutation Trp48 → Phe. Here, we present the first definitive evidence for a bridging, symmetrical peroxo adduct from vibrational spectroscopic studies of the freeze-trapped intermediate of this mutant R2. Isotope-sensitive bands are observed at 870, 499, and 458 cm^{−1} that are assigned to the intraligand peroxo stretching frequency and the asymmetric and symmetric Fe–O₂–Fe stretching frequencies, respectively. Similar results have been obtained in the resonance Raman spectroscopic study of a peroxodiferric species of Δ^9 -stearoyl-ACP desaturase [Broadwater, J. A., Ai, J., Loehr, T. M., Sanders-Loehr, J., and Fox, B. G. (1998) *Biochemistry* 37, 14664–14671]. Similarities among these adducts and transient species detected during O₂ activation by methane monooxygenase hydroxylase, ferritin, and wild-type protein R2 suggest the symmetrical peroxo adduct as a common intermediate in the diverse oxidation reactions mediated by members of this class.

Subunit R2 of ribonucleotide reductase (RNR)¹ contains a diiron center that activates oxygen for the production of the catalytically essential tyrosyl radical (1, 2). It belongs to a class of evolutionarily related proteins, including the hydroxylase component of soluble methane monooxygenase (MMOH) and Δ^9 stearoyl-acyl carrier protein desaturase (Δ^9 D), in which O₂ activation is thought to proceed through peroxo intermediates (3, 4). Recently, a relatively long-lived intermediate ($t_{1/2} \approx 0.75$ s at 5 °C) was detected in the O₂ reaction of a site-directed mutant R2 protein possessing the iron ligand substitution, Asp84 → Glu (5). The intermediate exhibits a broad absorption centered at 700 nm, which decays into bands at ~ 409 and $\sim 325/365$ nm characteristic of the tyrosyl radical and the oxidized [Fe–O–Fe]⁴⁺ center, respectively (5). Mössbauer analysis (5) of the 700 nm absorbing intermediate trapped by rapid freeze-quenching showed it to be diamagnetic with $\delta = 0.63$ mm/s and ΔE_Q

$= 1.58$ mm/s. These optical and Mössbauer properties are similar to those of a structurally characterized peroxodiiron(III) model complex (6) and the MMOH intermediate (designated compound P or H_{peroxo}) for which a similar structure has been proposed (7–10). On this basis, a peroxodiiron(III) structure was tentatively proposed for the R2–D84E intermediate. We have now obtained resonance Raman (RR) spectroscopic evidence proving this structural assignment in R2–W48F/D84E. We observe the vibration for $\nu(\text{O–O})$ at 870 cm^{−1}, and two Fe–O₂ vibrations at 458 and 499 cm^{−1}, assigned to ν_s and ν_{as} , respectively, that indicate that the peroxo group is bridging the two Fe(III) atoms. All three bands exhibit the expected isotope shifts in samples prepared with ¹⁷O₂ and ¹⁸O₂. Furthermore, the spectra of the intermediate prepared with mixed-isotope ¹⁶O¹⁸O show that the peroxo moiety is symmetrically coordinated, quite likely in a μ -1,2 fashion (see structures in Table 1). This study presents the first definitive vibrational spectroscopic identification of an intermediate O₂ adduct in a member of the nonheme diiron class of enzymes.

MATERIALS AND METHODS

Introduction of the W48F mutation into the *Escherichia coli nrdB* gene (encoding protein R2) has been described (11). The D84E mutation was introduced separately into the gene by using the polymerase chain reaction with the vector pR2wt–HindIII as template. This vector was constructed by modifying the previously described pR2–F208Y

[†] This work was supported by grants from the NIH [GM-18865 (T.M.L.) and GM-55365 (J.M.B.)], the NSF [BIR-9216592] for the Raman spectroscopy instrumentation at OGI, and the Searle Scholar's Program of the Chicago Community Trust and the Camille and Henry Dreyfus Foundation (J.M.B.).

* To whom correspondence should be addressed. E-mail: jmb21@psu.edu.

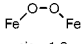
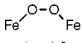
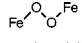
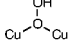
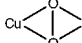
[‡] Joint first authors.

[§] Oregon Graduate Institute of Science and Technology.

^{||} The Pennsylvania State University.

¹ Abbreviations: Δ^9 D, Δ^9 stearoyl-acyl carrier protein desaturase; MMOH, hydroxylase component of soluble methane monooxygenase; RR, resonance Raman; RNR, ribonucleotide reductase.

Table 1: Raman Frequencies and Isotope Shifts in Peroxo Complexes^a

| peroxo species | $\nu_s(\text{M}-\text{O}_2)$ | $\nu_{as}(\text{M}-\text{O}_2)$ | $\nu(\text{O}-\text{O})$ | geometry |
|---|------------------------------|---------------------------------|--------------------------|---|
| R2 protein ^b | | | | |
| ¹⁶ O ₂ | 458 | 499 | 870 | Fe—O—O—Fe |
| ¹⁷ O ₂ , ¹⁶ O ¹⁸ O | (−8) | (−11) | (−23) ^c | μ -1,2 |
| ¹⁸ O ₂ | (−16) | (−22) | (−46) | |
| [Fe ₂ (μ -1,2-O ₂)(N-Et-HPTB)(Ph ₃ PO) ₂](BF ₄) ₃ ^d | | nr | |  |
| ¹⁶ O ₂ | 476 | | 900 ^c | μ -1,2 |
| ¹⁸ O ₂ | (−16) | | (−50) | |
| [Fe ₂ O(O ₂)(6-Me ₃ -TPA) ₂](ClO ₄) ₂ ^e | | nr | |  |
| ¹⁶ O ₂ | 462 ^c | | 848 | μ -1,2 |
| ¹⁸ O ₂ | (−21) | | (−46) | |
| [Fe ₂ (μ -O ₂)(μ -O ₂ CCH ₂ Ph) ₂ (HB(pz') ₃) ₂] ^f | | nr | |  |
| ¹⁶ O ₂ | 415 | | 888 | μ -1,2 |
| ¹⁸ O ₂ | (−11) | | (−46) | |
| [Cu ₂ (UN-O [−])(O ₂ H)](PF ₆) ₂ ^g | | | |  |
| ¹⁶ O ₂ | 322 | 506 | 892 | μ -1,1 |
| ¹⁸ O ₂ | (−10) | (−15) | (−52) | |
| oxyhemocyanin ^h | | | |  |
| ¹⁶ O ₂ | <i>i</i> | 542 | 749 | |
| ¹⁸ O ₂ | <i>i</i> | (−23) | (−40) | |

^a Frequencies in wave numbers; isotope shifts in parentheses relative to value for ¹⁶O₂; nr = not reported. ^b This work. ^c Indicates the center frequency of a Fermi resonance doublet. ^d Data from ref 17. ^e Data from ref 16. ^f Data from ref 6; similar frequencies of 429 (−12), nr, and 876 (−48) cm^{−1}, respectively, have been observed for the corresponding μ -benzoate complex (36). ^g Data from ref 37. ^h *Octopus dofleini* oxyhemocyanin data from ref 38. ⁱ The $\nu_s(\text{Cu}_2\text{O}_2)$ modes are admixed with Cu—N(His) modes (38).

(11) so as to revert codon 208 back to the wild-type but retain the translationally silent C to A mutation at the third position of codon 210. This introduces a unique *Hind*III restriction site to facilitate mutagenesis. Primers 1 (5'-GAAGTGGCGGAGCCCCGATCTTCCCC-3') and 2 (5'-GAATGGACTCGAGCAGCGTCTGATATTTTCAGG-3') were used to amplify the 480 bp fragment of pR2wt-*Hind*III containing the 218 bp of the template vector immediately 5' of the *nrdB* gene and bp 1–262 of the gene. Primers 3 (5'-GACGCTGCTCGAGTCCATTCAGGGTCGTAGCCC-3') and 4 (5'-GGAACAAGCAAAGCTTACGTAGAAACGAATCGC-3') were used to amplify the 406 bp fragment containing bp 243–648 of the gene. Primers 2 and 3 introduce two mutations into the overlapping PCR fragments: codon 84 is changed from GAT (encoding Asp) to GAG (encoding Glu), while codon 83 undergoes a silent change from CTG to CTC (both encoding Leu). As a result, codons 83 and 84 define a new *Xho*I restriction site, which was used to join the two PCR fragments. The larger fragment was restricted with *Bgl*II (which cuts 5' of the gene) and *Xho*I, the smaller fragment with *Xho*I and *Hind*III, and the pR2wt-*Hind*III vector with *Bgl*II and *Hind*III. The restricted PCR fragments and the large vector fragment were joined in a three-piece ligation, and the desired product (pR2-D84E) was identified by restriction analysis of plasmid DNA obtained from *E. coli* strain DH5 α cells that were transformed by the ligation mixture.

To construct the plasmid (pR2-W48F/D84E) encoding the double-mutant protein used in this study, the 268 bp *Bgl*II to *Aat*II restriction fragment (containing codons 1–52) from an R2 vector containing the W48F mutation (11) was joined with the large (vector) fragment from digestion of pR2-D84E with the same enzymes. The sequences of the coding regions of all plasmid vectors were verified to ensure that no unwanted mutations had been introduced during construction. Expression and purification of the mutant protein was carried out as previously described (11).

To prepare samples of the intermediate, an O₂-saturated solution of apo R2-W48F/D84E (1.8–2.1 mM in 100 mM

Hepes buffer, pH 7.6) was mixed at 5 \pm 2 °C by rapid flow with an equal volume of an O₂-saturated solution of Fe²⁺ (4 equiv relative to protein in 0.005 N H₂SO₄). From the mixer, the reaction solution flowed directly through an open-ended capillary (1 mm i.d. \times 4 cm), which was manually immersed into cold 2-methylbutane \sim 1 s after actuation of flow to yield samples with the intense blue color characteristic of the intermediate. Spectra were obtained on these frozen samples, which were kept at \sim 90 K with a liquid N₂ coldfinger (12). A 647.1 nm Kr⁺ laser was used for excitation. The backscattered light was analyzed with a custom McPherson 2061/207 spectrograph set to a focal length of 1 m and equipped with a 1800 grooves/mm grating, a Kaiser super-notch filter and a Princeton Instruments liquid-N₂ cooled (LN-1100PB) CCD detector. Laser power at the sample was \sim 250 mW for a total collection time of 3–4 h obtained by addition of separate 30 min exposures. The similarity of individual spectra and the visual observation of the distinct blue color of the peroxo intermediate confirmed the integrity of the sample after laser illumination. A featureless fluorescence background was subtracted from each spectrum using identical settings for data collection on the same preparations frozen after completion of the reaction. The data acquisition software WinSpec (Princeton Instruments) was used to collect the RR spectra. These data were exported as ASCII-XY files to GRAMS-386 (Galactic Industries Corp.) for linearization, calibration, and analysis. The spectral presentations were made with Origin (MicroCal).

RESULTS AND DISCUSSION

We and others have made extensive use of the rapid freeze-quench method to trap unstable intermediates in the O₂ reactions of the diiron proteins (13, 14). A potential disadvantage of this method as applied to resonance Raman spectroscopy is that the cryosolvent (typically 2-methylbutane) constitutes a significant fraction of the sample, and its Raman features may complicate detection of authentic, resonance-enhanced modes of intermediates.² To obviate the use of a cryosolvent, we further engineered the R2-D84E

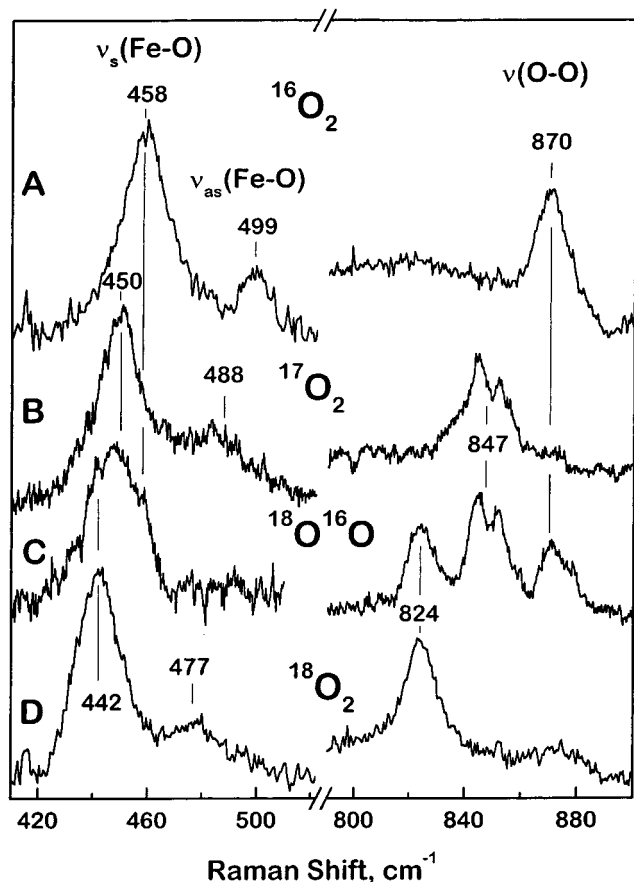


FIGURE 1: Resonance Raman spectra of the freeze-trapped peroxo intermediate of R2 generated with (A) $^{16}\text{O}_2$, (B) $^{17}\text{O}_2$ (85.5 at. % ^{17}O), (C) $^{16}\text{O}^{18}\text{O}$ mixture (50 at. % ^{18}O), and (D) $^{18}\text{O}_2$ gas (95 at. % ^{18}O). (Additional data obtained on a different composition of $^{16}\text{O}^{18}\text{O}$, and a mixed $^{16}\text{O}^{17}\text{O}^{18}\text{O}$ gas are not presented, although their analyses confirm our interpretation).

protein to confer greater kinetic stability to the putative peroxodiiron(III) intermediate. Substitution of tryptophan residue 48 with phenylalanine, which was previously shown to block electron transfer to the diiron cluster during O_2 activation (11), was found to increase the lifetime of the intermediate nearly 4-fold ($t_{1/2} \approx 2.7$ s at 5 °C).³ This additional stability was sufficient to allow the intermediate to be trapped by manual freezing in the absence of cryosolvent.

The resonance Raman spectrum of the intermediate prepared with $^{16}\text{O}_2$ (Figure 1A) consists of three isotope-sensitive bands at 870, 499, and 458 cm^{-1} . These bands could not be detected in control samples containing only the final products nor in the intermediate samples after thawing and refreezing. Moreover, the intensities of these vibrational bands were sensitive to the laser wavelength, being observed by excitation at 647.1 nm within the 700 nm absorption of the presumed peroxodiiron(III) complex, but lost when using a blue excitation. Comparison of the observed frequencies

and isotope shifts to those of μ -1,2 model systems (6, 16, 17; the crystal structure of the latter complex was reported in ref 18) supports the assignment of the 870 cm^{-1} band to $\nu(\text{O}-\text{O})$. The two lower frequency modes exhibit the correct frequency and intensity pattern as out-of-phase and in-phase $\text{Fe}-\text{O}_2-\text{Fe}$ stretching modes, respectively (Table 1) (19, 37). The existence of these symmetric and antisymmetric modes indicates that the peroxo group is coordinated to the diiron(III) center in a bridging fashion.

These three peaks shift by -46 , -22 , and -16 cm^{-1} , respectively, in the sample prepared with $^{18}\text{O}_2$ (Figure 1D). The magnitudes of these shifts are very close to the values expected for the mass effect of diatomic oscillators (-50 , -22 , -20 cm^{-1} , respectively). When the protein is reacted with a mixed-isotope dioxygen having a composition of 25:50:25 of $^{18}\text{O}_2$: $^{16}\text{O}^{18}\text{O}$: $^{16}\text{O}_2$, the resulting spectrum in the $\text{O}-\text{O}$ stretching region splits into a four-line pattern with relative intensity ratios of $\approx 1:1:1:1$ (Figure 1C). The splitting of the central peak into two nearly equal components might be considered indicative of an asymmetrically bound peroxo group (20, 21), as in an end-on or μ -1,1 geometry. However, further experiments did not support such a conclusion. A deuterium-isotope effect, which is expected for a protonated hydroperoxide, was not observed in RR spectra of samples prepared in D_2O . Moreover, when the intermediate was prepared with almost pure $^{17}\text{O}_2$, a similar splitting of $\nu(\text{O}-\text{O})$ around a centroid of 847 cm^{-1} was observed (Figure 1B).⁴ The appearance of this doublet from the symmetrically labeled $^{17}\text{O}_2$ complex proves that the splitting must arise from an effect distinct from the geometry of dioxygen binding. Rather, it may be ascribed to Fermi resonance between the $\text{O}-\text{O}$ stretch and an underlying mode not normally enhanced at this excitation wavelength. Fermi resonance has been reported previously for several peroxo-diiron(III) model complexes (see Table 1) to account for doublets in one isotopic composition becoming singlets in another (16, 17).

The intensity pattern of $\nu_s(\text{Fe}-\text{O})$ in the mixed-isotope spectrum (Figure 1C) confirms the symmetric bridging peroxo species, $\text{Fe}-\text{O}-\text{O}-\text{Fe}$, deduced from the $\nu(\text{O}-\text{O})$ region. The structured band consists of an intense, central peak at ~ 450 cm^{-1} , arising from the superimposed $\text{Fe}-^{18}\text{O}-^{16}\text{O}-\text{Fe}$ components, that is flanked by shoulders at 442 cm^{-1} ($\text{Fe}-^{18}\text{O}_2-\text{Fe}$) and 458 cm^{-1} ($\text{Fe}-^{16}\text{O}_2-\text{Fe}$). If the peroxo group had been asymmetrically coordinated to the two Fe atoms, the central peak would have been split and, consequently, of lower intensity than is observed here. This type of splitting has been observed in the asymmetric peroxo adducts of hemerythrin (20) and a dicopper model compound (22).

The copper complex, $[\text{Cu}_2(\text{UN}-\text{O}^-)(\text{O}_2\text{H})]^{2+}$, serves as a good model for the number of O_2 -sensitive vibrational modes in the R2 peroxo intermediate. Although its hydroperoxo ligand is believed to be bridging in a μ -1,1 rather than a μ -1,2 geometry, this complex exhibits an intraperoxo stretch at 892 cm^{-1} and two $\text{Cu}-\text{O}$ stretches of the $\text{Cu}-\text{OOH}-\text{Cu}$ unit assigned as the symmetric and asymmetric vibrations

² A resonance Raman feature initially ascribed to the putative peroxodiiron(III) adduct in MMOH (7) was later reported (15) to be an artifact arising, in part, from difficulties in the subtraction of the spectrum of 2-methylbutane cryosolvent used to prepare the freeze-quenched samples.

³ Under the conditions employed in this study, the 700 nm absorption feature of the intermediate develops with an apparent first-order rate constant (k_{obs}) of 2 ± 0.4 s^{-1} and decays with $k_{\text{obs}} = 0.26 \pm 0.02$ s^{-1} .

⁴ A mass spectroscopic composition of 85.5 at. % ^{17}O was provided by the vendor. Raman analysis of the gas gave three peaks corresponding to $^{16}\text{O}^{17}\text{O}$ ($\sim 10\%$), $^{17}\text{O}_2$ ($\sim 75\%$), and $^{17}\text{O}^{18}\text{O}$ ($\sim 15\%$). All O_2 isotopes were obtained from ICON Services, Summit, NJ.

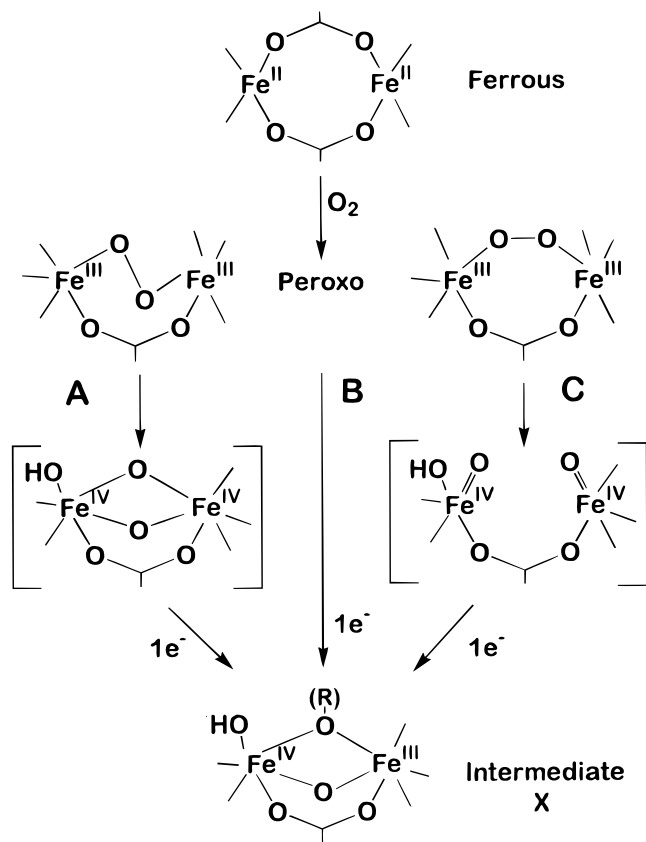


FIGURE 2: Possible reaction sequences for O₂ activation by protein R2 of RNR.

at 322 and 506 cm⁻¹, respectively (37) (Table 1). This system provides a precedent for the assignment of the *two* Fe—O stretches at 458 and 499 cm⁻¹ in the R2—W48F/D84E intermediate. The actual frequency of $\nu_s(\text{Fe—O}_2)$ in R2 at 458 cm⁻¹ is closest to the 462–476-cm⁻¹ range for *cis* μ -1,2 diiron peroxo complexes (Table 1). The alternative symmetric geometry of μ - η^2 : η^2 , as exhibited by oxyhemocyanin (23), can be ruled out in that the intraperoxo frequency in that system is at least 100 cm⁻¹ lower in energy (Table 1).

The symmetrically coordinated peroxo adduct (Figure 2) detected in R2—W48F/D84E is relevant to the O₂ reactions of several other diiron proteins. Data on $\Delta^9\text{D}$ indicate that it forms a similar μ -1,2 peroxo species, consisting of three isotope-sensitive RR bands at 898, 490, and 442 cm⁻¹, as discussed in the following article (24). This structure is also supported by the observation of a μ -1,3 azido complex in $\Delta^9\text{D}$ (25). As noted above, the putative peroxo adduct in MMOH has optical and Mössbauer properties that are extremely similar to those of the R2—W48F/D84E peroxo species (7–10). Likewise, some evidence suggests that a very fleeting intermediate with similar Mössbauer parameters forms in the O₂ reaction of the wild-type R2 protein (26). Finally, spectroscopic and kinetic analyses of the ferritin ferroxidase reaction also indicate a single transient formulated as a peroxodiferric species (14).

Possible mechanisms for O₂ activation by the diiron center of wild-type R2 are shown in Figure 2. The four-coordinate iron atoms in the diferrous structure of R2 have two bridging carboxyl groups (E115 and E238) and, in addition, each iron has one histidine and one monodentate carboxylate (D84, H118; E204, and H241) (27, 28). In mutant proteins

containing the D84E mutation, reaction with O₂ produces a peroxo intermediate, and the present data indicate that the O₂ is symmetrically bridged between the two Fe(III) ions. If the wild-type R2 protein also forms the peroxodiiron(III) species, it would imply that the simple addition of a methylene unit to the Asp84 ligand kinetically stabilizes the intermediate by more than 100-fold.⁵ In wild-type R2, the next intermediate that has been isolated, X, accumulates to near stoichiometry and is kinetically competent for tyrosyl 122 radical production (29). X is proposed to be a spin-coupled Fe(III)/Fe(IV) center containing a diamond core structure (30). One of the bridging oxo groups in the oxidized form of R2 (Y122F mutant) has been shown to be derived from O₂ (31). Other bridging oxygen atoms are either μ -O or μ -OR from water or carboxylates (30, 32). Preliminary evidence indicates that X does not accumulate in the reaction of R2—D84E, but this might result from changes in rate constants for constituent steps in the mechanism rather than from a change in the mechanism itself.

The stability of the peroxo species in R2—W48F/D84E and chemically reduced $\Delta^9\text{D}$ raises the question of whether these intermediates participate in the physiological reactions of these proteins. Assuming that a symmetrical μ -1,2 peroxo is involved, several reaction paths may be envisioned (Figure 2). Recent theoretical studies (33) suggest that a symmetrically bridging peroxo would readily undergo homolytic O—O bond cleavage resulting in an intermediate with each of the iron atoms at the Fe(IV) level. A *trans* μ -1,2 peroxo species (with an Fe—O—O—Fe dihedral angle close to 180°) could directly form a diamond core structure (Figure 2, path A) which has also been proposed for compound Q in MMOH (8–10, 34), whereas a *cis* μ -1,2 peroxo species (with a small dihedral angle) could produce a transient diferryl species (path C) that rearranges to the diamond core. Alternatively, compound X of R2 could be formed by direct one-electron reduction of the peroxide (35), followed by nuclear rearrangement (path B). This mechanism would provide explanation for the enhanced kinetic stability of the peroxo species associated with disruption of the electron-transfer pathway involving W48 (11). Irrespective of these important mechanistic details, it is likely that the diiron-carboxylate enzymes share a common initial pathway for O₂ activation including the formation of a bridging peroxo intermediate with a μ -1,2 coordination geometry.

ACKNOWLEDGMENT

We wish to thank Joann Sanders-Loehr for helpful advice in the discussion of experiments and the preparation of this manuscript. We also thank Ed Solomon and co-workers for sharing data of ref 37 prior to publication.

REFERENCES

1. Larsson, A., Karlsson, M., Sahlin, M., and Sjöberg, B. M. (1988) *J. Biol. Chem.* 263, 17780–17784.
2. Sjöberg, B.-M. (1997) *Struct. Bonding* 88, 139–173.

⁵ The peroxodiiron(III) intermediate in R2-D84E decays with a rate constant of 1 s⁻¹ (5), whereas the decay of the presumed peroxodiiron(III) intermediate in wild-type R2 has of lower limit of 130 s⁻¹ (B.A.L., and J.M.B., Jr., unpublished results).

3. Que, L., Jr., and Dong, Y. (1996) *Acc. Chem. Res.* 29, 190–196.
4. Wallar, B. J., and Lipscomb, J. D. (1996) *Chem. Rev.* 96, 2625–2657.
5. Bollinger, J. M., Jr., Krebs, C., Vicol, A., Chen, S., Ley, B. A., Edmondson, D. E., and Huynh, B. H. (1998) *J. Am. Chem. Soc.* 120, 1094–1095.
6. Kim, K., and Lippard, S. J. (1996) *J. Am. Chem. Soc.* 118, 4914–4915.
7. Liu, K. E., Valentine, A. M., Qiu, D., Edmondson, D. E., Appelman, E. H., Spiro, T. G., and Lippard, S. J. (1995) *J. Am. Chem. Soc.* 117, 4997–4998.
8. Shu, L., Nesheim, J. C., Kauffmann, K., Münck, E., Lipscomb, J. D., and Que, L., Jr. (1997) *Science* 275, 515–518.
9. Liu, K. E., Valentine, A. M., Wang, D., Huynh, B. H., Edmondson, D. E., Salifoglou, A., and Lippard, S. J. (1995) *J. Am. Chem. Soc.* 117, 10174–10185.
10. Liu, K. E., Wang, D., Huynh, B. H., Edmondson, D. E., Salifoglou, A., and Lippard, S. J. (1994) *J. Am. Chem. Soc.* 116, 7465–7466.
11. Parkin, S. E., Chen, S., Ley, B. A., Mangravite, L., Edmondson, D. E., Huynh, B. H., and Bollinger, J. M., Jr. (1998) *Biochemistry* 37, 1124–1130.
12. Loehr, T. M., and Sanders-Loehr, J. (1993) *Methods Enzymol.* 226, 431–470.
13. Huynh, B. H., Bollinger, J. M., Jr., and Edmondson, D. E. (1998) in *Spectroscopic Methods in Bioinorganic Chemistry* (Solomon, E. I., and Hodgson, K. O., Eds.) pp 403–422, American Chemical Society, Washington, DC.
14. Pereira, A. S., Small, W., Krebs, C., Tavares, P., Edmondson, D. E., Theil, E. C., and Huynh, B. H. (1998) *Biochemistry* 37, 9871–9876.
15. Liu, K. E., Valentine, A. M., Qiu, D., Edmondson, D. E., Appelman, E. H., Spiro, T. G., and Lippard, S. J. (1997) *J. Am. Chem. Soc.* 119, 11134.
16. Dong, Y., Zang, Y., Shu, L., Wilkinson, E. C., and Que, L., Jr. (1997) *J. Am. Chem. Soc.* 119, 12683–12684.
17. Dong, Y., Menage, S., Brennan, B. A., Elgren, T. E., Jang, H. G., Pearce, L. L., and Que, L., Jr. (1993) *J. Am. Chem. Soc.* 115, 1851–1859.
18. Dong, Y., Yan, S., Young, V. G., Jr., and Que, L., Jr. (1996) *Angew. Chem., Int. Ed. Engl.* 35, 618–620.
19. Mahroof-Tahir, M., Murthy, N. N., Karlin, K. D., Blackburn, N. J., Shaikh, S. N., and Zubieta, J. (1992) *Inorg. Chem.* 31, 3001–3003.
20. Kurtz, D. M., Jr., Shriver, D. F., and Klotz, I. M. (1976) *J. Am. Chem. Soc.* 98, 5033–5035.
21. Loehr, T. M. (1988) in *Oxygen Complexes and Oxygen Activation by Transition Metals* (Martell, A. E., and Sawyer, D. T., Eds.) pp 17–32, Plenum, New York.
22. Pate, J. E., Cruse, R. W., Karlin, K. D., and Solomon, E. I. (1987) *J. Am. Chem. Soc.* 109, 2624–2630.
23. Magnus, K. A., Hazes, B., Ton-That, H., Bonaventura, C., Bonaventura, J., and Hol, W. G. J. (1994) *Proteins* 19, 302–309.
24. Broadwater, J. A., Ai, J., Loehr, T. M., Sanders-Loehr, J., and Fox, B. G. (1998) *Biochemistry* 37, 14664–14671.
25. Ai, J., Broadwater, J. A., Loehr, T. M., Sanders-Loehr, J., and Fox, B. G. (1997) *J. Biol. Inorg. Chem.* 2, 37–45.
26. Tong, W. H., Chen, S., Lloyd, S. G., Edmondson, D. E., Huynh, B. H., and Stubbe, J. (1996) *J. Am. Chem. Soc.* 118, 2107–2108.
27. Regnström, K., Åberg, A., Örmö, M., Sahlin, M., and Sjöberg, B.-M. (1994) *J. Biol. Chem.* 269, 6355–6361.
28. Åberg, A. (1993) Ph.D. Dissertation, Stockholm University.
29. Bollinger, J. M., Jr., Edmondson, D. E., Huynh, B. H., Filley, J., Norton, J. R., and Stubbe, J. (1991) *Science* 253, 292–298.
30. Riggs-Gelasco, P. J., Shu, L., Chen, S., Burdi, D., Huynh, B. H., Que, L., Jr., and Stubbe, J. (1998) *J. Am. Chem. Soc.* 120, 849.
31. Ling, J., Sahlin, M., Sjöberg, B.-M., Loehr, T. M., and Sanders-Loehr, J. (1994) *J. Biol. Chem.* 269, 5595–5601.
32. Sturgeon, B. E., Burdi, D., Chen, S., Huynh, B.-H., Edmondson, D. E., Stubbe, J., and Hoffman, B. M. (1996) *J. Am. Chem. Soc.* 118, 7551–7557.
33. Yoshizawa, K., Ohta, T., Yamabe, T., and Hoffmann, R. (1997) *J. Am. Chem. Soc.* 119, 12311–12321.
34. Lee, S.-K., Fox, B. G., Froland, W. A., Lipscomb, J. D., and Münck, E. (1993) *J. Am. Chem. Soc.* 115, 6450–6451.
35. Bollinger, J. M., Jr., Chen, S., Parkin, S. E., Mangravite, L. M., Ley, B. A., Edmondson, D. E., and Huynh, B. H. (1997) *J. Am. Chem. Soc.* 119, 5976–5977.
36. Brunold, T. C., Tamura, N., Kitajima, N., Moro-oka, Y., and Solomon, E. I. (1998) *J. Am. Chem. Soc.* 120, 5674–5690.
37. Root, D. E., Mahroof-Tahir, M., Karlin, K. D., and Solomon, F. T. (1998) *Inorg. Chem.* 37, 4838–4848.
38. Ling, J., Nestor, L. P., Czernuszewicz, R. S., Spiro, T. G., Fraczkiewicz, R., Sharma, K. D., Loehr, T. M., and Sanders-Loehr, J. (1994) *J. Am. Chem. Soc.* 116, 7682–7691.

BI981838Q